AIR POLLUTION OVER THE GANGES BASIN AND NORTH-WEST BAY OF BENGAL IN THE EARLY POST-MONSOON SEASON BASED ON NASA MERRAERO DATA

Pavel Kishcha,

Department of Geophysical, Atmospheric and Planetary Sciences, Tel-Aviv University, 69978 Tel-Aviv, Israel

Arlindo M. da Silva

Global Modeling and Assimilation Office, NASA/GSFC, Greenbelt, Maryland USA.

Boris Starobinets

Department of Geophysical, Atmospheric and Planetary Sciences, Tel-Aviv University, 69978 Tel-Aviv, Israel

Pinhas Alpert

Department of Geophysical, Atmospheric and Planetary Sciences, Tel-Aviv University, 69978 Tel-Aviv, Israel

Journal of Geophysical Research – Atmospheres,

Accepted for publication on January 13, 2014

Abstract

The MERRA Aerosol Reanalysis (MERRAero) has been recently developed at NASA's Global Modeling Assimilation Office (GMAO). This reanalysis is based on a version of the GEOS-5 model radiatively coupled with GOCART aerosols, and it includes assimilation of bias-corrected Aerosol Optical Thickness (AOT) from the MODIS sensor on both Terra and Aqua satellites. In October over the period 2002-2009, MERRAero showed that AOT was lower over the east of the Ganges basin than over the north-west of the Ganges basin: this was despite the fact that the east of the Ganges basin should have produced higher anthropogenic aerosol emissions because of higher population density, increased industrial output and transportation. This is evidence that higher aerosol emissions do not always correspond to higher AOT over the areas where the effects of meteorological factors on AOT dominate those of aerosol emissions. MODIS AOT assimilation was essential for correcting modeled AOT mainly over the north-west of the Ganges basin, where AOT increments were maximal. Over the east of the Ganges basin and north-west BoB, AOT increments were low and MODIS AOT assimilation did not contribute significantly to modeled AOT. Our analysis showed that increasing AOT trends over north-west BoB (exceeding those over the east of the Ganges basin) were reproduced by GEOS-5, not because of MODIS AOT assimilation, but mainly because of the model capability of reproducing meteorological factors contributing to AOT trends. Moreover, vertically integrated aerosol mass flux was sensitive to wind convergence causing aerosol accumulation over north-west BoB.

1. Introduction

The Indian subcontinent (and the Ganges basin in particular) is characterized by a significant population growth accompanied by developing industry, agriculture, and increasing transportation. This has resulted in declining air quality [Di Girolamo et al. 2004, Ramanathan and Ramana, 2005, Tripathi et al., 2005, Prasad and Singh, 2007, Kaskaoutis et al., 2011a, Dey and Di Girolamo, 2011, Krishna Moorthy et al., 2013]. With respect to air pollution, one could suggest some relationship between population figures and anthropogenic aerosol emissions. Indeed, Kishcha et al. [2011] showed that, over extensive areas with differing population densities in the Indian subcontinent, the higher the averaged population density – the larger the averaged AOT. In addition, the larger the population growth - the stronger the increasing AOT trends.

In accordance with Di Girolamo et al. [2004], Prasad and Singh [2007], Kumar et al. [2010], prevailing winds blowing along the Ganges basin in the post-monsoon and winter months transport anthropogenic aerosol particles into the Bay of Bengal. A number of sea expeditions to BoB were conducted to investigate the resulting increased levels of air pollution over BoB [Ramachandran and Jayaraman, 2003; Vinoj et al., 2004; Ganguly et al., 2005, Moorthy et al., 2008, Kumar et al., 2010, Kaskaoutis et al., 2011b]. Moreover, long-term AOT trends over South Asia, including BoB, were examined, using different satellite AOT data sets, by Mishchenko and Geogdzhayev [2007], Zhao et al. [2008], Zhang and Reid [2010], Kaskaoutis et al. [2011a], Dey and Di Girolamo [2011], and Hsu et al. [2012]. Based on AVHRR satellite data, Mishchenko and Geogdzhayev [2007] compared over-water AOT averaged over two separate periods, 1988–1991 and 2002–2005, and found significant changes. Zhao et al. [2008] studied AOT trends over the whole area of BoB for spring, summer, autumn, and winter during the 25-year period 1981 – 2005, using AVHRR data. Using MODIS-Terra Level 2 AOT data, Zhang and Reid [2010] analyzed AOT trends over the whole area of BoB for all months during the 10-year period 2000 - 2009. The spatial distribution of decadal (2000 – 2009) MODIS Level-3 AOT trends over South Asia, including BoB, in different months was obtained by Kaskaoutis et al. [2011a]. Using MISR aerosol data, decadal (2000 – 2009) AOT trends over the Indian subcontinent and surrounding sea areas were also estimated by Dey and Di Girolamo [2011]. Hsu et al.

[2012] created maps of SeaWiFS AOT trends over the period 1998 – 2010 for each of the four seasons.

The early post-monsoon season over the study region is characterized by aerosol transport from the Ganges basin to north-west BoB by prevailing winds; and still significant rainfall of over 150 mm/month over the east of the Ganges basin and north-west BoB. It would be reasonable to consider that AOT trends over sea areas in BoB were created by changes in aerosol sources on the land in the Indian subcontinent. In our previous study [Kishcha et al., 2012], we found that it was not always the case. Specifically, we found that, in October, MODIS showed strong increasing aerosol optical thickness (AOT) trends over north-west Bay of Bengal (BoB) in the absence of AOT trends over the east of the Indian subcontinent. This was unexpected, because sources of anthropogenic pollution were located over the Indian subcontinent, mainly in the Ganges basin, and aerosol transport from the Indian subcontinent to north-west BoB was carried out by prevailing winds.

It was our purpose to determine whether existing state-of-the-art aerosol data-assimilated systems were capable of reproducing the aforementioned AOT trends over north-west BoB in the early post-monsoon season, in the presence of significant rainfall. For the model, it would be a challenge just to obtain correct space-time distribution of rainfall, which is of importance for estimating aerosol wet removal. The NASA Goddard Earth Observing System (GEOS-5) was used to extend the NASA Modern Era-Retrospective Analysis for Research and Applications (MERRA) reanalysis by adding five atmospheric aerosol components (sulfates, organic carbon, black carbon, desert dust, and sea-salt). In the current study, the obtained eight-year (2002 – 2009) assimilated aerosol dataset (so-called MERRAero) was applied to examine aerosol trends over the Ganges basin and north-west Bay of Bengal (BoB) in the post-monsoon season. In addition, using air pollution modeling allowed us to look at the situation over the study region from the point of view of air quality. This was carried out by estimating the contribution of various aerosol species to AOT and its trends.

Note that AOT assimilation was effective only for two short periods of MODIS's appearance over the study area. All other times (18 hours per day) the GEOS-5 model worked independently of MODIS.

2. GEOS-5 and the MERRA Aerosol Reanalysis (MERRAero)

2.1 GEOS-5 Earth Modeling System

GEOS-5 is the latest version of the NASA Global Modeling and Assimilation Office (GMAO) Earth system model. GEOS-5 contains components for atmospheric circulation and composition (including atmospheric data assimilation), ocean circulation and biogeochemistry, and land surface processes. Components and individual parameterizations within components are coupled under the Earth System Modeling Framework (ESMF) [Hill et al., 2004]. In addition to traditional meteorological parameters (winds, temperatures, etc. [Rienecker et al., 2008]), GEOS-5 includes modules representing the atmospheric composition, most notably aerosols [Colarco et al., 2010], and tropospheric/stratospheric chemical constituents [Pawson et al., 2008], and the impact of these constituents on the radiative processes of the atmosphere.

2.2 Aerosols in GEOS-5

GEOS-5 includes modules representing atmospheric composition, including aerosols [Colarco et al., 2010] and tropospheric and stratospheric chemical constituents [Pawson et al., 2008]. The current generation aerosol module is based on a version of the Goddard Chemistry, Aerosol, Radiation, and Transport (GOCART) model [Chin et al., 2002]. GOCART treats the sources, sinks, and chemistry of dust, sulfate, sea salt, and black and organic carbon aerosols. Aerosol species are assumed to be external mixtures. Both dust and sea salt have wind-speed dependent emission functions [Colarco et al., 2010], while sulfate and carbonaceous species have emissions principally from fossil fuel combustion, biomass burning, and bio-fuel consumption, with additional biogenic sources of organic carbon. Sulfate has additional chemical production from oxidation of SO2 and dimethylsulfide (DMS), as well as a database of volcanic SO2 emissions and injection heights. Aerosol emissions for sulfate and carbonaceous species are based on the AeroCom version 2 hindcast inventories [Dr. Thomas Diehl, personal communication, and http://aerocom.met.no/emissions.html). Daily biomass burning emissions are from the Quick Fire Emission Dataset (QFED) and are derived from MODIS fire radiative power retrievals [Darmenov and da Silva, 2013]. Total mass of sulfate and carbonaceous aerosols are tracked, while for dust and sea salt the particle size distribution is explicitly resolved across five non-interacting size bins for each.

For all aerosol species, optical properties are primarily from the commonly used Optical Properties of Aerosols and Clouds (OPAC) data set [Hess et al., 1998]. OPAC provides the spectrally varying refractive index and a humidification factor for each aerosol species which, together with assumptions about the particle size distribution of each species, are used to construct spectrally varying lookup tables of aerosol optical properties such as the mass extinction efficiency, single scattering albedo, and asymmetry parameter, inputs required by our radiative transfer codes (details are in Colarco et al. [2010], and references therein).

2.3 GEOS-5 Data Assimilation

GEOS-5 has a mature atmospheric data assimilation system that builds upon the Grid-point Statistical Interpolation (GSI) algorithm, jointly developed with NCEP [Wu et al. 2002, Derber et al. 2003, Rienecker et al. 2008]. The GSI solver was originally developed at NCEP as an unified 3D-Var analysis system for supporting global and regional models. GSI includes all the in-situ and remotely sensed data used for operational weather prediction at NCEP.

GEOS-5 also includes assimilation of AOT observations from the MODIS sensor on both Terra and Aqua satellites. Based on the work of Zhang and Reid [2006] and Lary [2009], a back-propagation neural network has been developed to correct observational biases related to cloud contamination, surface parameterization, aerosol microphysics, etc. On-line quality control is performed with the adaptive buddy check of Dee et al. [2001], with observation and background errors estimated using the maximum likelihood approach of Dee and da Silva [1999].

2.4 MERRA Aerosol (MERRAero) Reanalysis

MERRA is a NASA reanalysis for the satellite era using a major new version of the Goddard Earth Observing System Data Assimilation System Version 5 (GEOS-5) [Rienecker et al., 2011]. The Project focuses on historical analyses of the hydrological cycle from the NASA EOS suite of observations in a climate context, on a broad range of weather and climate time scales and places. The MERRA time period covers the modern era of remotely sensed data, from 1979 through the present, and the special focus of the atmospheric assimilation is the hydrological cycle. Like other similar reanalysis, MERRA provides meteorological parameters (winds, temperature, humidity), along with a number of other diagnostics such as surface and top of the atmosphere fluxes, diabatic terms and the observational corrections imposed by the data assimilation procedure.

As a step toward an Integrated Earth System Analysis (IESA), the GMAO is producing several parallel re-analyses of other components of the earth system such as ocean, land and atmospheric composition. Of particular relevance for this paper the MERA Aerosol Reanalysis (MERRAero), where MODIS AOT observations are assimilated providing a companion aerosol gridded datasets that can be used to study the impact of aerosols on the atmospheric circulation and on air quality in general. Table 1 summarizes the main attributes of MERRAero. Notice that MERRAero only covers the later years of MERRA, capitalizing on the improved aerosol measurements from NASA's EOS platforms.

3. Method

Following our previous study [Kishcha et al., 2012], we analyzed long-term variations of AOT over seven zones, each 3^o x 3^o, located in the Ganges basin and north-west BoB (Fig. 1). As mentioned, in the post-monsoon period, prevailing winds blow along the Ganges basin. The specified zones in the Ganges basin provide us with an opportunity for analyzing air pollution trends produced by local sources and aerosol transport. Fig. 1a shows the spatial distribution of eight-year mean MERRAero AOT over the region under consideration in October, together with the location of zones 3^o x 3^o in the Indian subcontinent (zone 1 to zone 5) and in the Bay of Bengal (zones 6 and 7). MERRAero monthly AOT data are available from the year 2002. To analyze AOT and its trends over the Indian subcontinent and north-west BoB, we used monthly MERRAero AOT data with horizontal resolution of approximately 50 km, during the eight-year period 2002 – 2009. To estimate the NASA GEOS-5 model performance, 3-hour MERRAero AOT data together with AOT increments were used.

A linear fit was used to determine the resulting trend of aerosol optical thickness during the study period (2002 – 2009) over each of the aforementioned zones. The obtained AOT trend values correspond to the slope of the linear fit. To ensure that the linear fit produced normally distributed residuals, they were required to pass the Shapiro–Wilk normality test [Shapiro and Wilk, 1965, Razali and Wah, 2011]. If the residuals were normally distributed, they could be used in a t-test, in order to estimate the statistical significance of a linear fit. The statistical significance of the AOT trend was checked by applying the significance level (p) value, i.e. $p < 0.05$ for statistically significant AOT trends at the 95 % confidence level.

4. Results

4.1. Total MERRAero AOT and its trends in October

In accordance with spatial distribution of eight-year mean AOT in the early post-monsoon season (October), MERRAero showed high AOT values over the Ganges basin with a maximum over the north-west part of the Ganges basin (Fig. 1a). Therefore, MERRAero data were able to reproduce the main structure of aerosol distribution over the Ganges basin. The Ganges basin is the most polluted part of the Indian subcontinent, where highly-populated areas and main industrial centers are located.

We analyzed zone-to-zone variations of MERRAero AOT averaged over the specified zones. In the early post-monsoon season (October), MERRAero showed mainly decreasing AOT variations from zone 3 to zone 5 (Fig. 2a and Table 2). Note that this decrease in AOT from north-west to east of the Ganges basin does not correspond to the distribution of population density: population density is higher in the east of the Ganges basin (zones 4 and 5) than in the north-west of the Ganges basin (zone 1) (Fig. 3). At first glance, this is contradictory to our previous findings on the relationship between

AOT and population density in the Indian subcontinent [Kishcha et al., 2011]. It should be mentioned, however, that, in our previous study, we used averaging over significant areas of the Indian subcontinent with differing population densities.

The most probable reason for the decrease in AOT over the east of the Ganges basin, where population density is the highest in the entire Ganges basin, is wet removal processes after significant rainfall in October. Monthly accumulated Tropical Rainfall Measuring Mission (TRMM) rainfall data from the 3B42V6 archive, on a $0.25^o \times 0.25^o$ latitude-longitude grid [Huffman et al., 2007], were used to estimate zone-to-zone variations of eight-year (2002 – 2009) mean TRMM rainfall over the specified zones in October (Fig. 4a). High rainfall values of over 150 mm can be seen in October over the east of the Ganges basin (zone 5) and north-west BoB (zone 6). Moreover, rainfall data showed that, over the east of the Ganges basin, the accumulated rainfall in October in the first four-year period 2002 – 2005 was essentially higher than in the second four-year period 2006 – 2009 (Fig. 4a). As a result, higher values of MERRAero AOT over the east of the Ganges basin (zones 4 and 5) were observed in the second four-year period 2006 – 2009 than in the first four-year period 2002 – 2005 (Fig. 2b). Moreover, the aforementioned decrease in the eight year (2002 – 2009) mean AOT over the east of the Ganges basin and north-west BoB in October corresponds to the increase in model-simulated aerosol wet deposition over the specified zones towards north-west BoB, in accordance with the spatial distribution shown in Fig. 4b.

Therefore, we have arrived at the interesting point, which is as follows. The east of the Ganges basin should have produced higher anthropogenic aerosol emissions than the north-west of the Ganges basin because of higher population density, increased industrial output and transportation. Nevertheless, MERRAero showed that AOT over the east of the Ganges basin was lower than that over the north-west of the Ganges basin. This is evidence that higher aerosol emissions do not always correspond to higher AOT. This can take place over the areas where the effects of meteorological factors on AOT (in this case, precipitation) dominate those of aerosol emissions.

Spatial distributions of MERRAero AOT trends during the eight-year (2002 – 2009) study period showed strong increasing AOT trends over north-west BoB exceeding those over the Ganges basin (Fig. 1b). This indicates that MERRAero is capable of reproducing the main features of the phenomenon of strong increasing AOT trends over north-west BoB in the early post-monsoon season, in line with our previous study [Kishcha et al., 2012].

4.2. Effects of rainfall on MERRAero AOT

As mentioned, in the early post-monsoon season (October), intense rainfall can be frequently observed over the east of the Ganges basin. These severe precipitation events could strongly affect AOT over the east of the Ganges basin due to aerosol wet removal processes. To understand the rain effects on AOT over the east of the Ganges basin (zone 5), we compared year-to-year variations of assimilated MERRAero AOT and TRMM accumulated rainfall, over zone 5 in each October during the study period (not shown). Rainfall data showed that the accumulated rainfall in October in the first four-year period 2002-2005 was higher than in the second four-year period 2006-2009. A strong inverse relationship (with a high negative correlation of over -0.8) between changes in assimilated MERRAero AOT and rainfall is clearly seen: each increase in rainfall was accompanied by a decrease in assimilated AOT. The aforementioned decrease in rainfall over zone 5 in October during the study period can explain some increasing trend in MERRAero AOT observed over that area in October (Table 2). There was some dissimilarity in the rainfall amount between the east of the Ganges basin (zone 5) and north-west BoB (zone 6): north-west BoB does not show as clear decreasing trends in rainfall amount as the east of the Ganges basin does.

4.3. AOT of different aerosol species and their trends in the early post-monsoon season

As known, satellite remote sensing data can not distinguish between various aerosol species. MERRAero provides us with an opportunity to look at the situation over the study region from the point of view of air quality. This was carried out by estimating the contribution of various aerosol species to AOT and its trends. Based on MERRAero model data, Fig. 5a represents zone-to-zone variations of eight-year (2002 – 2009) mean AOT of several aerosol components (desert dust; organic and black carbon; and sulfates) averaged over specified zones in October, and their trends. One can see that over the west of the Ganges basin (zones 1 - 3), where precipitation was minimal (Fig. 4a), each aerosol component changes from zone to zone in a different way, in accordance with its own emissions, transport, and gravitational settling (Fig. 5a). By contrast, over the east of the Ganges basin (zones 4 - 5), a general decrease in AOT can be observed due to increasing aerosol wet removal towards north-west BoB (Fig. 4b). Over zone 1, there is a considerable amount of carbon aerosols (as a result of crop waste burning [Sharma et al., 2010]), dust particles, and sulfate aerosols (Fig. 5a). This explains the AOT maximum over the north-west of the Ganges basin in October. Over sea areas (zones 6 – 7), aerosols are dominated by anthropogenic air pollution, such as sulfates and carbon aerosols (Fig. 5a). This predominance can affect cloud formation, atmospheric dynamics, and even marine life in this region.

By contrast to sulfates and carbonates, dust aerosol particles have no sources along the Ganges basin. Therefore, dust distribution along the Ganges basin is determined by aerosol transport (by the action of prevailing winds blowing along the Ganges basin) and by deposition processes. One can see that the eight-year mean dust AOT values noticeably decreased along the Ganges basin and over north-west BoB. This resulted in the decrease in dust contribution to the total AOT from approximately 30% over zone 1 to 8% over zones from 5 to 7 (Table 3). Furthermore, dust AOT trends did not change in transition from land to sea: approximately the same slightly increasing dust AOT trends of ~0.004 yr-1 were obtained along the east of the Ganges basin and over north-west BoB (Figs. 5b and 6c). We found that these AOT trends over zones from 5 to 7 were statistically significant (Table 3). The same dust AOT trends along the Ganges basin and over north-west BoB suggest an increasing trend in some external source of dust emissions, outside the Ganges basin. It should be kept in mind that MERRAero only assimilates total AOT and that the trend in aerosol speciation may depend on the trend (or lack thereof) of the specified emissions.

The distribution of sulfate AOT along the Ganges basin is determined by sulfate aerosol emissions, together with aerosol transport (by the action of prevailing winds) and deposition processes (Fig. 5a). The sulfate contribution to the total AOT increased along the Ganges basin from approximately 30 % over zone 1 to ~56% over zone 5 (Table 3). Over north-west BoB (zones 6 and 7), the sulfate contribution to the total AOT was over 50% (Table 3). Thus, according to MERRAero AOT data, sulfates were the major atmospheric aerosol component over the east of the Ganges basin and over north-west BoB. Moreover, MERRAero data showed that sulfate AOT trends changed in transition from land to sea: strong statistically-significant increasing sulfate AOT trends (of 0.008

yr^{-1} and 0.011 yr^{-1} over zones 6 and 7 respectively) exceeded those over the east of the Ganges basin (zone 5) (Figs. 5b and 6a, and Table 3).

With respect to organic and black carbon aerosols, their distribution of eight-year mean AOT values along the Ganges showed a wide maximum from the north-west to the center of the Ganges basin (zones from 1 to 3) (Fig. 5a). As mentioned, this area of maximum carbon AOT is known for crop waste burning aerosols [Sharma et al., 2010. Venkataraman et al., 2006]. AOT values of carbon aerosols decrease to the east from zone 3 (Fig. 5a). As discussed in Section 4.1, the reason for the decrease in AOT over the east of the Ganges basin in October is significant rainfall accompanied by aerosol wet removal processes. The joint contribution of organic and black carbon aerosols to the total AOT is ~38% over the north-west of the Ganges basin (zones from 1 to 3); ~35% over the east of the Ganges basin (zone 5), and approximately 27% over north-west BoB (zones 6 and 7) (Table 3). Similar to AOT trends of sulfate aerosols, MERRAero showed that AOT trends of carbon aerosols changed in transition from land to sea: increasing AOT trends in organic and black carbon AOT over the sea (zones 6 and 7) exceeded those over zone 5 in the land (Fig. 5b and 6b, and Table 3).

Based on MERRAero data, we found that, in October, the contribution of sea-salt aerosols to the total AOT over the east of the Ganges basin was even lower than that of desert dust. Over north-west BoB, desert dust and sea-salt aerosols equally contributed to the total AOT (Fig. 7a). Our analysis showed that sea-salt aerosols did not contribute to the increasing AOT trends over north-west BoB: no sea-salt AOT trend was observed in year-to-year variations during the study period (Fig. 7a). This was supported by year-to-year variations of MERRA surface winds over north-west BoB (Fig. 7b).

4.4. Factors contributing to AOT trends over north-west BoB

MERRAero showed increasing AOT trends over north-west BoB in October exceeding AOT trends over the east of the Ganges basin (Fig. 1b). This was despite the fact that sources of air pollution are located on the land, mainly in the Ganges basin. There could be several factors contributing to the increasing AOT trends over north-west BoB. First, there were changes in the atmospheric circulation over north-west BoB in October during the eight-year study period (Fig. 8). Mean wind vectors of the 700-850 hPa layer in each October during the 8-year period under consideration were analyzed (Fig. 8).

The 700-850 hPa layer is considered as indicative of wind in the lower troposphere, where aerosol transport mainly occurs [Dunion and Velden, 2004]. During the second 4-year period (2006 – 2009), prevailing winds blowing mainly from land to sea (Fig. 8, e - h) resulted in a drier environment and less precipitation over the east of the Ganges basin and north-west BoB (Fig. 4a) than during the first 4-year period (2002 – 2005) (Fig. 8, a - d). This caused less wet removal of air pollution in the second 4-year period than in the first 4-year period. Second, our analysis showed that, during the eight-year study period, there was an increasing number of days (Np, in percentage form) in each October when prevailing winds blew from land to sea (Fig. 9). This suggests some increasing trends in the transport of anthropogenic air pollution from their sources in the east of the Ganges basin to north-west BoB. Third, for Octobers when Np > 50%, wind convergence was observed over north-west BoB causing the accumulation of aerosol particles over that region (Fig. 10), in line with our previous study [Kishcha et al., 2012]. All the three factors contributed to the increasing AOT trend over north-west BoB in the early post-monsoon season.

Fig. 11 represents maps of the absolute value of the magnitude of monthly vertically integrated mass flux of aerosols including sulfates, carbonates, and desert dust over the study region. These maps were obtained for each October between 2002 and 2009. One can see that, over north-west BoB (zone 6), the aerosol flux was higher during the second 4-year period (2006 – 2009) (when prevailing winds blew mainly from land to sea) than during the first 4-year period (2002 – 2005) (when prevailing winds blew frequently from sea to land). In October 2009, monthly mean wind over zone 6 was minimal (less than 1 m/s) (Fig. 8h). As the aerosol flux is proportional to wind, then one could expect that the aerosol flux over zone 6 should be also minimal. However, as shown in Fig. 11h, in October 2009, the aerosol flux over zone 6 was maximal during the study period. The maximal flux under the minimal wind indicates accumulating aerosol particles over zone 6. This is supported by the analysis of wind convergence: the wind convergence over zone 6 was also maximal in October 2009 (Fig. 10e). Therefore, we can conclude that vertically integrated aerosol mass flux is sensitive to wind convergence causing aerosol accumulation. Moreover, the aerosol flux is sensitive to precipitation: its magnitude is maximal over the north-west of the Ganges basin, and decreases towards north-west BoB over the specified zones in the east of the Ganges basin, due to wet removal processes after significant rainfall (Fig. 11). Therefore, the analysis of aerosol fluxes supports our findings on the effects of wind convergence and precipitation on AOT.

5. Analysis of AOT increments

MODIS crosses the study area twice a day. Specifically, MODIS-Terra crosses the study area at approximately 04:30 UT (10:30 LT), while MODIS-Aqua at approximately 08:30 UT (14:30 LT). MODIS-Terra AOT retrievals were used for updating MERRAero AOT at 6 UT, while MODIS-Aqua retrievals were used for updating MERRAero AOT at 9 UT. It is clear that, after the two consecutive updates, MERRAero AOT at 9 UT corresponds in the best way to available MODIS measurements over the study area. During all other times (18 hours per day), the model simulates air pollution over the study area independently of MODIS, using available meteorology and predefined aerosol emissions. Taking into account the uncertainty of aerosol emissions over such a complex study area, which includes the highly-populated and polluted Ganges basin, one could expect some accumulation of model errors in AOT simulations during the 18-hour period without data assimilation.

We estimated the NASA GEOS-5 model performance over the study area analyzing model AOT increments. These AOT increments are the field differences between MODIS AOT and modeled AOT. AOT increments include a complex combination of all model errors in AOT simulations over each specific location. To analyze AOT increments, 3-hour MERRAero AOT data were used. These 3-hour data allowed us to distinguish between 3-hour periods with and without MODIS AOT assimilation. Fig. 12a represents a spatial distribution of the eight year (2002 – 2009) mean AOT increments at 6 UT. One can see maximal AOT increments over the north-west of the Ganges basin (zones 1 – 3), where precipitation was minimal as shown in Fig. 4a. In the absence of precipitation, the deficiency in anthropogenic aerosol emissions could be the main contributor to the high AOT increments. By contrast, over the east of the Ganges basin and north-west BoB (zones 4 – 7), AOT increments were low, indicating that MODIS AOT assimilation did not contribute significantly to modeled AOT there. This was despite the fact that, in the east of the Ganges basin (zones 4 – 5), the population density is the highest in the entire Ganges basin (Fig. 3), which means the highest industrial and transportation emissions. The most probable reason why AOT increments were lower over zones 4 – 5 than over zones 1 – 3, is the aforementioned significant increase in rainfall (accompanied by aerosol wet removal processes) towards north-west BoB. Over the east of the Ganges basin and north-west BoB, the NASA GEOS-5 model was capable of reproducing the effect of significant rainfall on MERRAero AOT which, in turn, dominates the effect of aerosol emissions there.

Fig. 12b represents a spatial distribution of the eight year (2002 – 2009) mean AOT increments at 9 UT. One can see that, in spite of the MODIS AOT assimilation at 6 UT, the AOT increments at 9 UT are quite significant over the north-west of the Ganges basin (zones 1 – 2). Therefore, MODIS AOT assimilations at 6 UT and 9 UT were essential for correcting modeled AOT mainly over the north-west of the Ganges basin, where AOT increments were maximal. Over the east of the Ganges basin and north-west BoB where AOT increments were low, MODIS AOT assimilation did not contribute significantly to modeled AOT.

Our findings are further illustrated by Fig. 13 which represents a comparison between spatial distributions of eight-year (2002 – 2009) AOT trends at 6 UT with and without AOT assimilation. Here, the modeled AOT without MODIS assimilation was obtained as the field difference between MODIS AOT and AOT increments at 6 UT. One can see some similarity in the two distributions of AOT trends, namely, AOT trends over north-west BoB exceed those over the Ganges basin (Fig. 13). This is evidence that the increasing AOT trends over north-west BoB were reproduced by the model not only because MODIS AOT assimilation provided us with an opportunity to correct the uncertainty in aerosol emissions, but mainly because the model was capable of reproducing changes in meteorological factors contributing to the AOT trends.

6. Conclusions

The recently developed eight-year (2002 – 2009) MERRAero assimilated aerosol data set was applied to the study of AOT and its trends over the Ganges basin and north-west BoB in the early post-monsoon season. MERRAero showed that AOT was lower over the east of the Ganges basin than over the north-west of the Ganges basin: this was despite the fact that the east of the Ganges basin should have produced higher anthropogenic aerosol emissions due to higher population density, increased industrial output and transportation. This is evidence that higher aerosol emissions do not always correspond to higher AOT over the areas where the effects of meteorological factors on AOT dominate those of aerosol emissions.

Based on the analysis of model AOT increments, we have arrived at the important point of the current study which is as follows: the decrease in AOT over the east of the Ganges basin towards north-west BoB was reproduced by the model not only because of MODIS AOT assimilation, but mainly because of the model capability of reproducing meteorological factors contributing to AOT. MODIS AOT assimilation was essential over the north-west of the Ganges basin, where AOT increments were maximal, indicating the deficiency in anthropogenic aerosol emissions used in the model. Over the east of the Ganges basin and north-west BoB, AOT increments were low and AOT assimilation did not contribute significantly to modeled AOT there.

In October, in the absence of aerosol sources in north-west BoB, MERRAero showed increasing AOT trends over north-west BoB exceeding those over the east of the Ganges basin. Similar AOT trends were obtained using MERRAero AOT with and without MODIS AOT assimilation. Various aerosol components showed strong increasing AOT trends over north-west BoB. Therefore, using MERRAero AOT, we obtained similar results with respect to AOT trends over north-west BoB, as in our previous study based on MODIS data [Kishcha et al., 2012].

There were a number of meteorological factors contributing to the increasing AOT trends over north-west BoB:

- an increasing number of days in each October when prevailing winds blew from land to sea, resulting in an increase in air pollution over north-west BoB;
- during the second 4-year period (2006 – 2009), prevailing winds blowing mainly from land to sea were responsible for a drier environment with less precipitation causing less wet removal of air pollution than in the first 4-year period (2002 – 2005);
- in October 2009, the vertically integrated aerosol mass flux over north-west BoB (zone 6) was maximal, while monthly mean wind was minimal. This indicates accumulating aerosol particles over north-west BoB. The wind convergence over north-west BoB was also maximal in October 2009. Therefore, vertically

integrated aerosol mass flux is sensitive to wind convergence causing aerosol accumulation.

The MERRAero AOT data set allowed us to determine aerosol species responsible for the AOT maximum over the north-west of the Ganges basin, which are both natural aerosols (dust particles) and anthropogenic aerosols (carbon aerosols from bio-mass burning and sulfates). In accordance with MERRAero data, most of dust particles fell out due to gravitational settling and wet deposition during dust transport from the north-west to the east of the Ganges basin. As a result, over the east of the Ganges basin and north-west BoB in the early post-monsoon season, aerosols were dominated by anthropogenic air pollution, such as sulfates and carbon aerosols. Our analysis showed that sea-salt aerosols did not contribute to the increasing AOT trends over north-west BoB: no sea-salt AOT trend was observed in year-to-year variations during the study period.

We used MERRAero aerosol reanalysis over the Ganges basin and north-west BoB, but this global NASA product can be used over other places. Our findings illustrate that, while analyzing MERRAero AOT over other places, model AOT increments could be helpful in determining (a) areas where effects of aerosol emissions on AOT dominate those of meteorology, and MODIS AOT assimilation would be essential for correcting modeled AOT, and (b) areas where effects of meteorological factors on AOT dominate those of aerosol emissions, and MODIS AOT assimilation would not contribute significantly to modeled AOT.

References

Chin, M., P. Ginoux, S. Kinne, O. Torres, B. Holben, B.N. Duncan, R.V. Martin, J. Logan, A. Higurashi, T. Nakajima (2002), Tropospheric aerosol optical thickness from the GOCART model and comparisons with satellite and sun photometer measurements. *J. Atmos. Phys*. 59, 461–483, doi: http://dx.doi.org/10.1175/1520-0469(2002)059.

Colarco, P., A. da Silva, M. Chin, and T. Diehl (2010), Online simulations of global aerosol distributions in the NASA GEOS-4 model and comparisons to datellite and ground-based aerosol optical depth. *J. Geophys. Res*., 115, D14207, doi:10.1029/2009JD012820.

Darmenov, A., and A.M. da Silva (2013), The quick fire emissions dataset (QFED) - Documentation of versions 2.1, 2.2 and 2.4. NASA Technical Report Series on Global Modeling and Data Assimilation. NASA TM-2013-104606, 32, 183p.

Dee, D.P., L. Rukhovets, R. Todling, A.M. da Silva, and J.W. Larson (2001), An Adaptive Buddy Check for Observational Quality Control. *Quarterly Journal of the Royal Meteorological Society,* 127(577), 2451–2471, doi:10.1002/qj.49712757714.

Dee, D.P., and A.M. da Silva (1999), Maximum-Likelihood Estimation of Forecast and Observation Error Covariance Parameters. Part I: Methodology. *Mon. Weather Rev.*, 127(8), 1822–1834, doi:http://dx.doi.org/10.1175/1520-0493.

Derber, J. C., R.J. Purser, W.-S. Wu, R. Treadon, M. Pondeca, D. Parrish, and D. Kleist (2003), Flow-dependent Jb in a global grid-point 3D-Var. *Proc. ECMWF annual seminar on recent developments in data assimilation for atmosphere and ocean.* Reading, UK, 8-12 Sept. 2003.

Dey, S., and L. Di Girolamo (2011), A decade of change in aerosol properties over the Indian subcontinent, *Geophys. Res. Lett.,* 38, L14811, doi:10.1029/2011GL048153.

DI Girolamo, L., T.C. Bond, D. Bramer, D.J. Diner, F. Fettinger, R.A. Kahn, J.V. Matronchik, M.V. Ramanathan, and P.J. Rash (2004), Analysis of Multi-angle Imaging SpectroRadiometer (MISR) aerosol optical depths over greater India during winter 2001 – 2004. *Geophys. Res. Lett.*, 31, L23115, doi:10.1029/2004GL021273.

Dunion, J. P., and C. S. Velden (2004), The impact of the Saharan air layer on Atlantic tropical cyclone activity, *Bull. Am. Meteorol. Soc*., 85(3), 353– 365, doi:10.1175/BAMS-85-3-353.

Ganguly, D., A. Jayaraman, and H. Gadhavi (2005), In situ ship cruise measurements of mass concentration and size distribution of aerosols over Bay of Bengal and their radiative impacts. *J. Geophys. Res*., 110, D06205, doi:10.1029/2004JD005325.

Hess, M, P Koepke, and I Schult (1998), Optical Properties of Aerosols and Clouds: the Software Package OPAC. *Bulletin of the American Meteorological Society,* 79 (5), 831–844, DOI:10.1175/1520-0477(1998)079.

Hill, C, C. DeLuca, Balaji, M. Suarez, and A. da Silva (2004): The architecture of the Earth System Modeling Framework. *Computing in Science and Engineering*, 6(1), 18–28.

Hsu, N.C., R. Gautam, A.M. Sayer, C. Bettenhausen, C. Li, M.J. Jeong, S.C. Tsay, and B.N. Holben (2012), Global and regional trends of aerosol optical depth over land and ocean using SeaWiFS measurements from 1997 to 2010.

Atmos. Chem. Phys. Discuss., 12, 8465-8501, doi:10.5194/acpd-12-8465-2012.

Huffman, G.J., R.F. Adler, D.T. Bolvin, G. Gu, E.J. Nelkin, K.P. Bowman, Y. Hong, E.F. Stocker, D.B. Wolff (2007), The TRMM multisatellite precipitation analysis (TMPA): quasi-global, multiyear, combined-sensor precipitation estimates at fine scales. *J. Hydrometeorology*, 8, 38 – 55, doi: 10.1175/JHM560.1.

Kaskaoutis, D.G., S.K. Kharol, P.R. Sinha, R.P. Singh, K.V.S. Badarinath, W. Mehdi, and M. Sharma (2011a). Contrasting aerosol trends over South Asia during the last decade based on MODIS observations. *Atmos. Meas. Tech. Discuss*., 4, 5275–5323, doi:10.5194/amtd-4-5275-2011.

Kaskaoutis, D.G., S. Kumar Kharol, P.R. Sinha, R.P. Singh, H.D. Kambezidis, A. Rani Sharma, and K.V.S. Badarinath (2011b), Extremely large anthropogenic aerosol contribution to total aerosol load over the Bay of Bengal during winter season. *Atmos. Chem. Phys.,* 11, 7097–10 7117, doi:10.5194/acp-11-7097-2011.

Kishcha, P., B. Starobinets, O. Kalashnikova, and P. Alpert (2011), Aerosol optical thickness trends and population growth in the Indian subcontinent. *Int. J. Remote. Sens.,* 32, 9137-9149, doi:10.1080/01431161.2010.550333.

Kishcha, P., B. Starobinets, C.N. Long, P. Alpert (2012), Unexpected increasing AOT trends over north-west Bay of Bengal in the early post-monsoon season. *J. Geophys. Res*., 117, D23208, doi 10.1029/2012JD018726.

Krishna Moorthy, K., S. Suresh Babu, M.R. Manoj, and S.K. Satheesh (2013), Buildup of aerosols over the Indian region. *Geophys. Res. Lett*., doi:10.1002/GRL.50165.

Kumar, A., M.M. Sarin, and B. Srinivas (2010), Aerosol iron solubility over Bay of Bengal: Role of anthropogenic sources and chemical processing, *Marine Chemistry*, 121, 167–175.

Lary, D.J., L.A. Remer, D. MacNeill, B. Roscoe, and S Paradise (2009), Machine Learning and Bias Correction of MODIS Aerosol Optical Depth. *Geoscience and Remote Sensing Letters*, IEEE, 6(4), 694–698, doi: 10.1109/LGRS.2009.2023605.

Mishchenko, M. I., and I. V. Geogdzhayev (2007), Satellite remote sensing reveals regional tropospheric aerosol trends, Opt. Express, 15, 7423 – 7438, doi:10.1364/OE.15.007423.

Moorthy, K.K., S.K. Satheesh, S.S. Babu, and C.B.S. Dutt (2008), Integrated campaign for aerosols, gases and radiation budget (ICARB): An overview. *J. Earth Syst. Sci*., 117, 243–262, doi:10.1007/s12040-008-0029-7.

Pawson, S., R.S Stolarski, A.R. Douglass, P.A. Newman, J.E.c Nielsen, S.M. Frith, and M.L Gupta (2008), Goddard Earth Observing System Chemistry-Climate Model Simulations of Stratospheric Ozone-Temperature Coupling Between 1950 and 2005. *J. Geophys. Res.*, 113(D12), D12103, doi:10.1029/2007JD009511.

Prasad, A.K. and R.P. Singh (2007), Comparison of MISR-MODIS aerosol optical depth over the Indo-Gangetic basin during the winter and summer seasons (2000-2005). *Remote Sensing of Environment*, 107, 109 – 119, doi:10.1016/j.rse.2006.09.026.

Ramachandran, S. and A. Jayaraman (2003), Spectral aerosol optical depths over Bay of Bengal and Chennai: II – Sources, anthropogenic influence and model estimates. *Atmos. Env.,* 37, 1951–1962, doi:10.1016/S1352-2310(03)00082-7.

Ramanathan, V., and M. Ramana (2005), Persistent, widespread and strongly absorbing haze over the Himalayan foothills and the Indo-Gangetic plains. *Pure and Applied Geophysics*, 162, 1609 – 1626, doi:10.1007/s00024-005-2685-8.

Razali, N.M., and Y.B. Wah (2011), Power comparisons of Shapiro-Wilks, Kolmogorov-Smirnov, Lilliefors and Anderson-Darling tests. *J. Statistical Modeling and Analytics,* 2, 21-33.

Rienecker, MM, MJ Suarez, R Todling, J Bacmeister, L Takacs, H-C Liu, W Gu, M. Sienkiewicz, R.D. Koster, R. Gelaro, I. Stajner, and E. Nielsen (2008), The GEOS-5 Data Assimilation System--Documentation of Version 5.0.1, 5.1.0, and 5.2.0. NASA/TM-2007-104606, 27, 1-118.

Rienecker, M.M., M.J. Suarez, R. Gelaro, R. Todling, J. Bacmeister, E. Liu, M.G. Bosilovich, S.D. Schubert, L. Takacs, G.-K. Kim, S. Bloom, J. Chen, D. Collins, A. Conaty, A. da Silva, et al. (2011), MERRA: NASA's Modern-Era Retrospective Analysis for Research and Applications. *J. Climate*, 24, 3624-3648, doi: 10.1175/JCLI-D-11-00015.1.

Shapiro, S.S., and M.B. Wilk (1965), An analysis of variance test for normality (complete samples). Biometrika, 52, 591 – 611, doi:10.1093/biomet/52.3-4.591.

Sharma, A.R., S.K. Kharol, K.V.S. Badarinath, and D. Singh (2010), Impact of agriculture crop residue burning on atmospheric aerosol loading – a study over Punjab State. India, *Ann. Geophys.*, 28, 367–379, doi:10.5194/angeo-28-367-2010.

Tripathi, S.N., S. Day, A. Chandel, S. Srivastava, R.P. Singh, and B. Holben (2005), Comparison of MODIS and AERONET derived aerosol optical depth over the Ganga basin, India. *Ann. Geophys.*, 23, 1093-1101, doi:10.5194/angeo-23-1093-2005.

Venkataraman, C., G. Habib, D. Kadamba, M. Shrivastava, J.-F., Leon, B. Crouzille, O. Boucher, D. Streets (2006), Emissions from open biomass burning in India: Integrating the inventory approach with high-resolution Moderate Resolution Imaging Spectroradiometer (MODIS) active-fire and land cover data. *Global Biogeochem. Cycles*, 20, GB2013, doi:10.1029/2005GB002547.

Vinoj, V., S.S. Babu, S.K. Satheesh, K.K. Moorthy, and Y.J. Kaufman (2004), Radiative forcing by aerosols over the Bay of Bengal region derived from shipborne, island-based, and satellite (Moderate-Resolution Imaging Spectroradiometer) observations. *J. Geophys. Res.*, 109, D05203, doi:10.1029/2003JD004329.

Wu, W.S., R.J. Purser, and D.F. Parrish (2002): Three-dimensional variational analysis with spatially inhomogeneous covariances. *Mon. Weather. Rev.*, 130, 2905–2916, doi:http://dx.doi.org/10.1175/1520-0493.

Zhang, J. and J.S. Reid (2006), MODIS Aerosol Product Analysis for Data Assimilation: Assessment of Over-Ocean Level 2 Aerosol Optical Thickness Retrievals. *J. Geophys. Res.*, 111(D22), D22207. doi:10.1029/2005JD006898.

Zhang, J.L. and J.S. Reid (2010), A decadal regional and global trend analysis of the aerosol optical depth using a data-assimilation grade over-water MODIS and Level 2 MISR aerosol products. *Atmos. Chem. Phys.*, 10, 10949-10963, doi:10.5194/acp-10-10949-2010.

Zhao, T. X.-P., I. Laszlo, W. Guo, A. Heidinger, C. Cao, A. Jelenak, D. Tarpley, and J. Sullivan (2008), Study of long-term trend in aerosol optical thickness observed from operational AVHRR satellite instrument, J. Geophys. Res., 113, D07201, doi:10.1029/2007JD009061.

Acknowledgements. This study was made with support from and in cooperation with the international Virtual Institute DESERVE (Dead Sea Research Venue), funded by the German Helmholtz Association. We also acknowledge the GES-DISC Interactive Online Visualization and Analysis Infrastructure (Giovanni) for providing us with TRMM data.

Table 1. The overview of main attributes of NASA MERRAero assimilated aerosol data.

Feature	Description
Model	GEOS-5 Earth Modeling System (with GOCART aerosol components); Constrained by MERRA Meteorology (Replay) Land sees obs. precipitation (like MERRA*Land*) Driven by QFED daily Biomass Emissions
Aerosol data assimilation	Local Displacement Ensembles (LDE) MODIS reflectances AERONET Calibrated AOT's (Neural Net) Stringent cloud screening
Period	mid 2002-present (Aqua + Terra)
Resolution	Horizontal: nominally 50 km Vertical: 72 layers, top ~85 km
Aerosol Species	Dust, sea-salt, sulfates, organic & black carbon

Table 2. Eight-year (2002-2009) mean AOT (τ), standard deviation (sd), and AOT slope (α) of MERRAero AOT averaged over the specified zones in October[υ].

Area	Zone #	Geographic Coordinates	τ	sd	α (per year)	S – W test	p
IS	1	28.5N – 31.5N 72.7E – 75.7E	0.53	0.07	-0.005	Normal	Not significant
	2	27N – 30N 75.7E – 78.7E	0.50	0.08	-0.004	Normal	Not significant
	3	25N – 28N 78.7E–81.7E	0.51	0.08	0.008	Normal	Not significant
	4	24N – 27N 82.5E–85.5E	0.43	0.05	0.012	Normal	Not significant
	5	22N – 25N 86E – 89E	0.35	0.05	0.010	Normal	Not significant
BoB	6	18N – 21N 87E – 90E	0.22	0.05	0.015	Normal	0.043
	7	15N – 18N 84E – 87E	0.20	0.05	0.020	Normal	0.006

[υ]The decision based on the Shapiro – Wilk normality test for residuals (S-W test) and the significance level (p) are also displayed. If the p value was too high as compared with the 0.05 significance level, the obtained linear fit was considered as statistically insignificant.

Table 3. The eight-year mean AOT (τ), standard deviation (sd), and AOT slope (α) for long-term changes of MERRAero AOT for different aerosol species (desert dust; organic and black carbon; and sulfates) averaged over specified zones in October. F corresponds to the fraction of aerosol component AOT (in percentages) from the total MERRAero AOT.

Area	Zone #	F %	τ	sd	α (per year)	S – W test	p
					Sulfates		
IS	1	31.7	0.17	0.04	0.001	Normal	Not significant
	2	36.7	0.18	0.04	-0.001	Normal	Not significant
	3	43.7	0.22	0.05	0.004	Normal	Not significant
	4	49.7	0.22	0.04	0.006	Normal	Not significant
	5	55.9	0.20	0.03	0.004	Normal	Not significant
BoB	6	52.9	0.12	0.03	0.008	Normal	0.050
	7	50.7	0.10	0.03	0.011	Normal	0.004
					Organic and black carbon		
IS	1	37.7	0.20	0.05	-0.011	Normal	Not significant
	2	39.2	0.20	0.03	-0.009	Normal	Not significant
	3	37.7	0.19	0.02	-0.001	Normal	Not significant
	4	37.5	0.16	0.02	0.002	Normal	Not significant
	5	34.9	0.12	0.02	0.003	Normal	Not significant
BoB	6	28.8	0.06	0.02	0.004	Normal	Not significant
	7	25.9	0.05	0.02	0.005	Normal	0.026
					Desert dust		
IS	1	29.5	0.16	0.04	0.006	Normal	Not significant
	2	23.2	0.12	0.03	0.006	Normal	Not significant
	3	17.8	0.09	0.03	0.005	Normal	Not significant
	4	12.2	0.05	0.02	0.004	Normal	Not significant
	5	8.0	0.03	0.01	0.004	Normal	0.035
BoB	6	8.3	0.02	0.01	0.004	Normal	0.012
	7	8.1	0.02	0.01	0.004	Normal	0.008

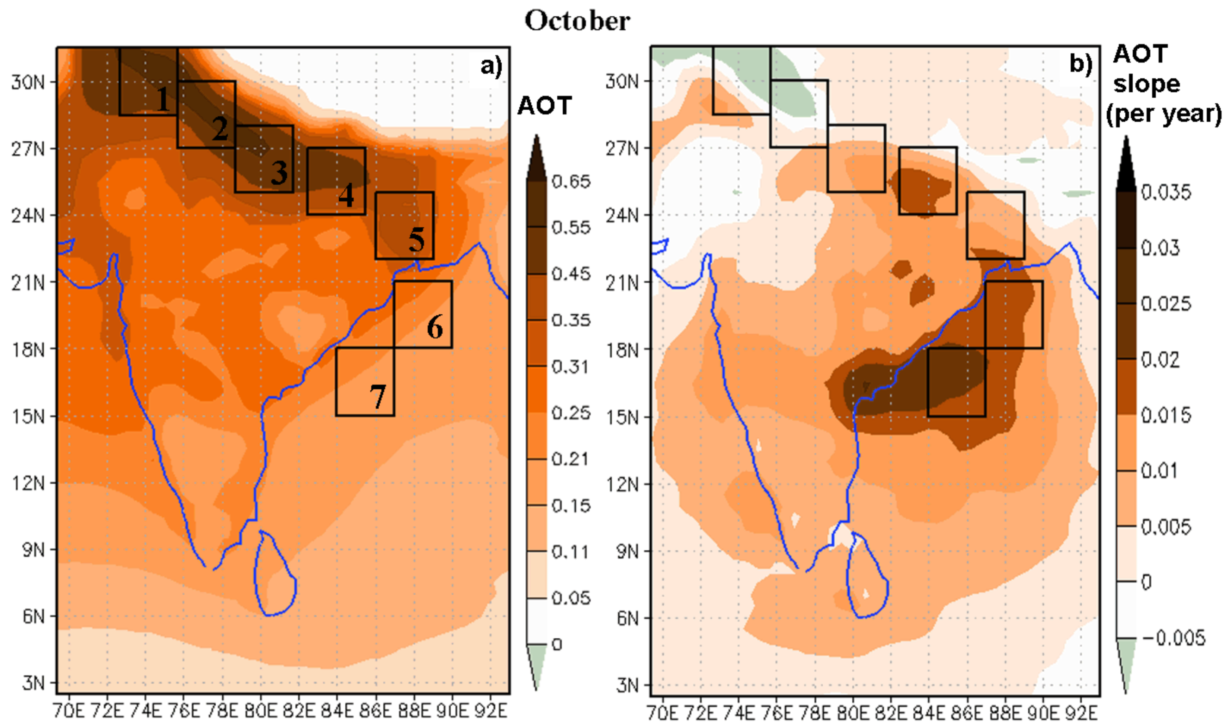

Figure 1. Spatial distributions of (a) the eight year (2002 – 2009) mean MERRAero AOT and (b) its trends (characterized by AOT slopes) in October. The AOT trend values correspond to the slope of the linear regression analysis. The squares show the locations of zones 1 to 7 within the study region.

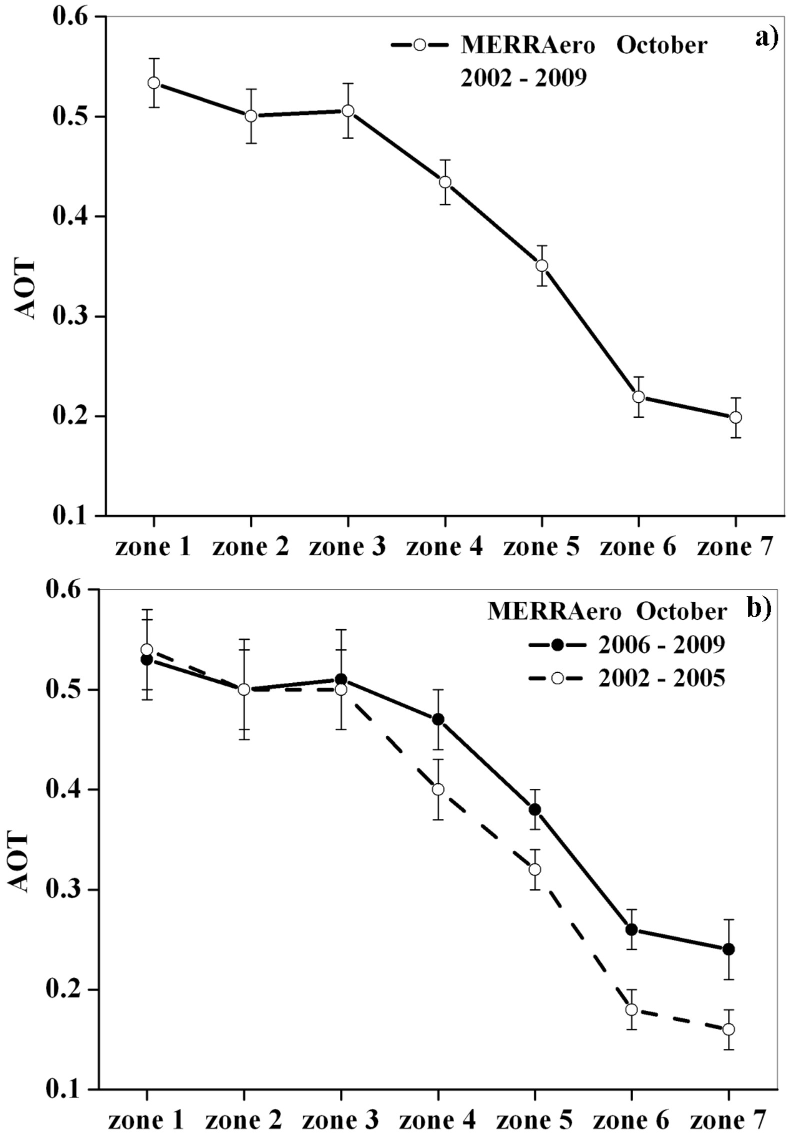

Figure 2. a - zone-to-zone variations of eight-year (2002-2009) mean MERRAero AOT averaged over the specified zones. b - zone-to-zone variations of MERRAero AOT averaged over the first four-year (2002-2005) period and over the second four-year (2006-2009) period. The error bars show the standard error of mean AOT.

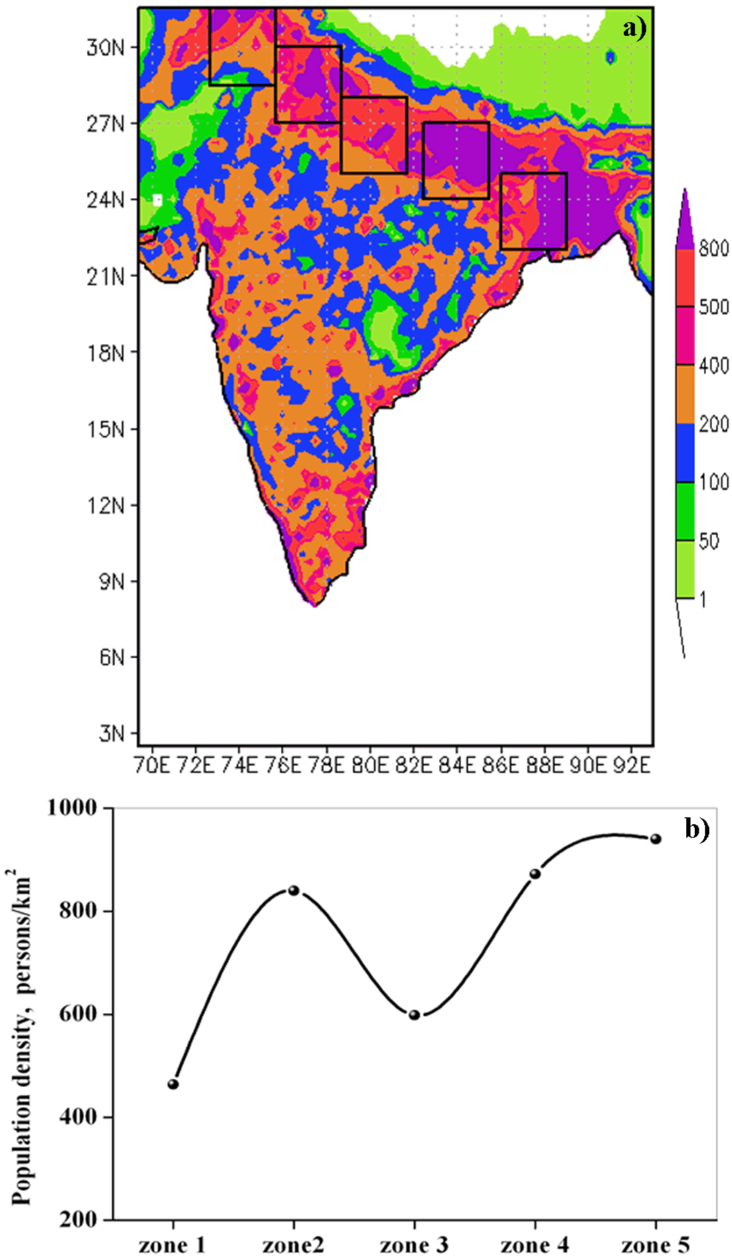

Figure 3. a – population density (persons km^{-2}) distributions over the Indian subcontinent. b – zone-to-zone variations of population density averaged over the specified zones. The GPW-v3 gridded population density data for the year 2005 were used (http://sedac.ciesin.columbia.edu/data/collection/gpw-v3).

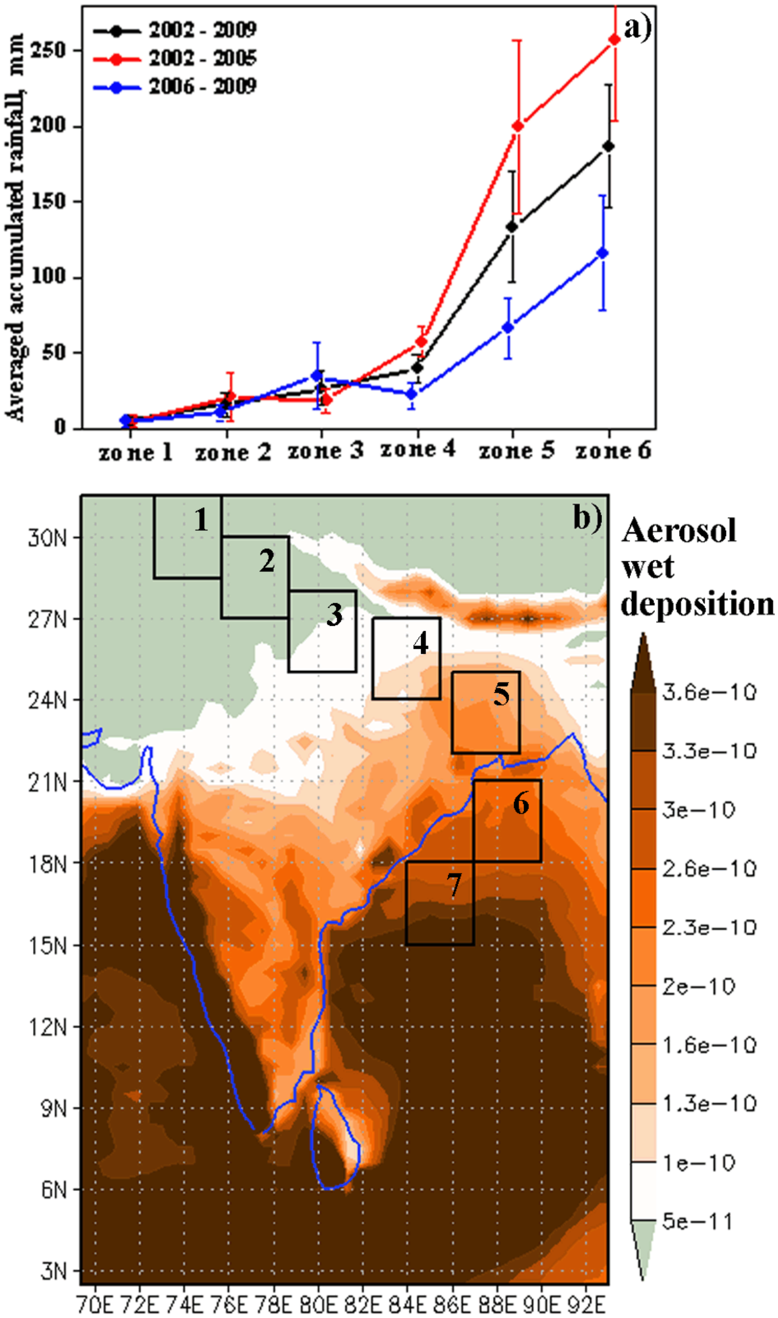

Figure 4. a - zone-to-zone variations of TRMM accumulated rainfall over the specified zones in October averaged over the eight-year study period (2002 – 2009), over the first 4-year period (2002 – 2005), and over the second 4-year period (2006 – 2009). The error bars show the standard error of mean accumulated rainfall. TRMM data from the 3B42V6 archive were used.

b – the spatial distribution of the eight year (2002 – 2009) mean model-simulated aerosol wet deposition rate (kg m^{-2} s^{-1}) in October.

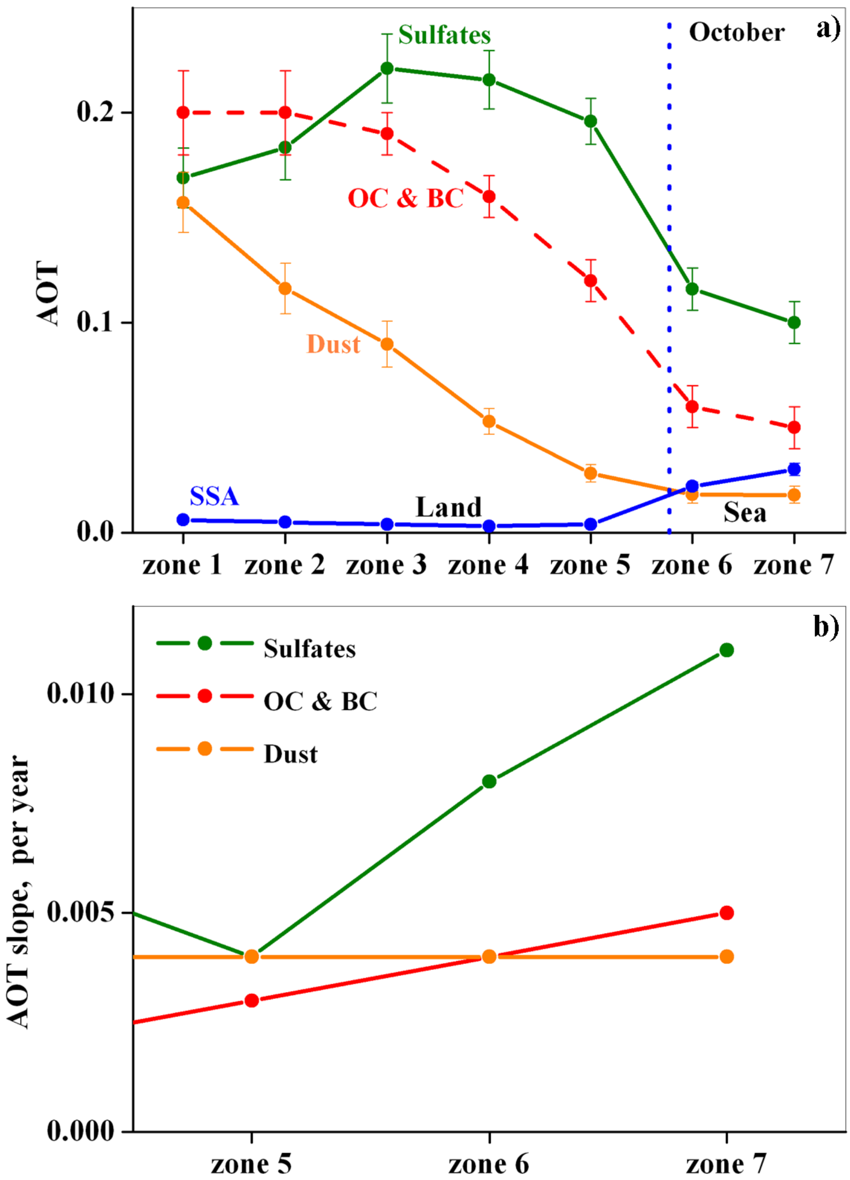

Figure 5. Zone-to-zone variations of (a) eight-year (2002-2009) mean MERRA AOT of various aerosol species (sulfates (SU), organic and black carbon (OC & BC), and desert dust) averaged over the specified zones in October, and (b) their AOT trends (characterized by the slope of the linear regression analysis). The error bars show the standard error of mean AOT.

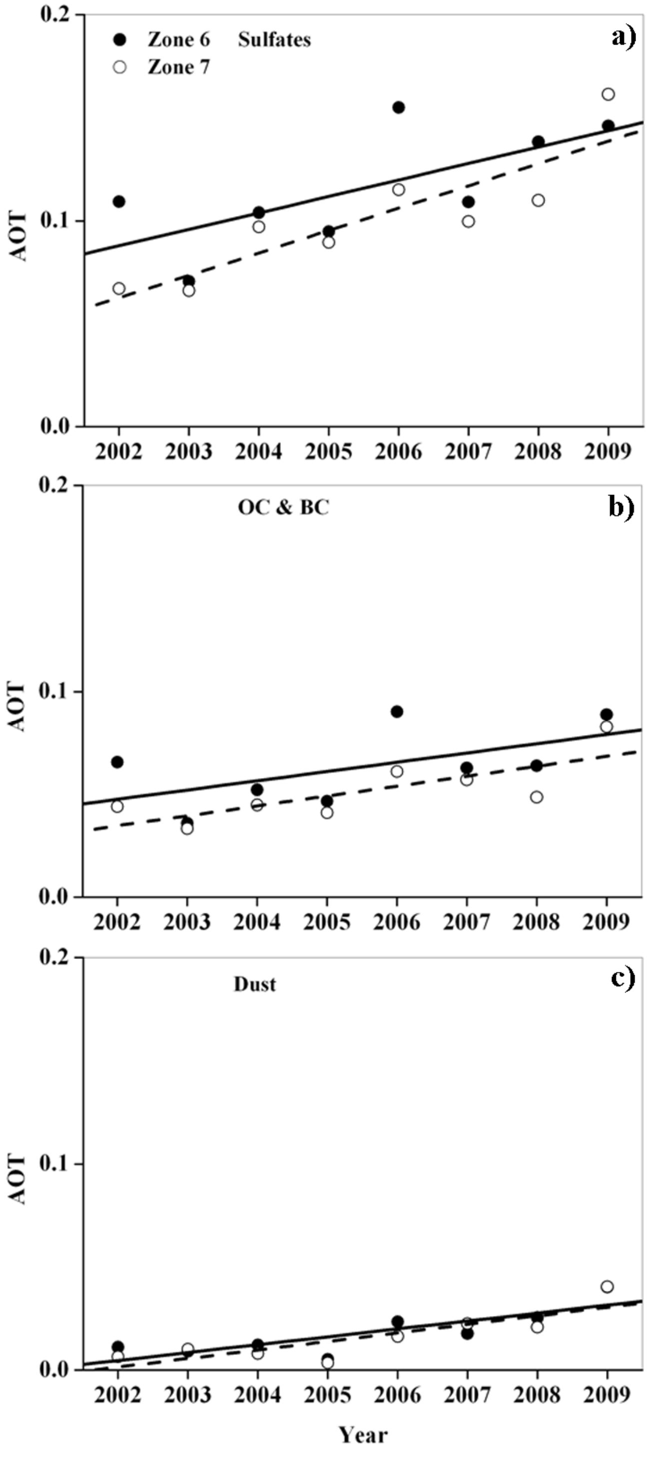

Figure 6. Year-to-year variations of AOT for various aerosol species (such as sulfates, organic carbon, and desert dust) over zones 6 and 7 in north-west BoB in October. The straight lines (dashed for zone 7 and solid for zone 6) designate linear fits.

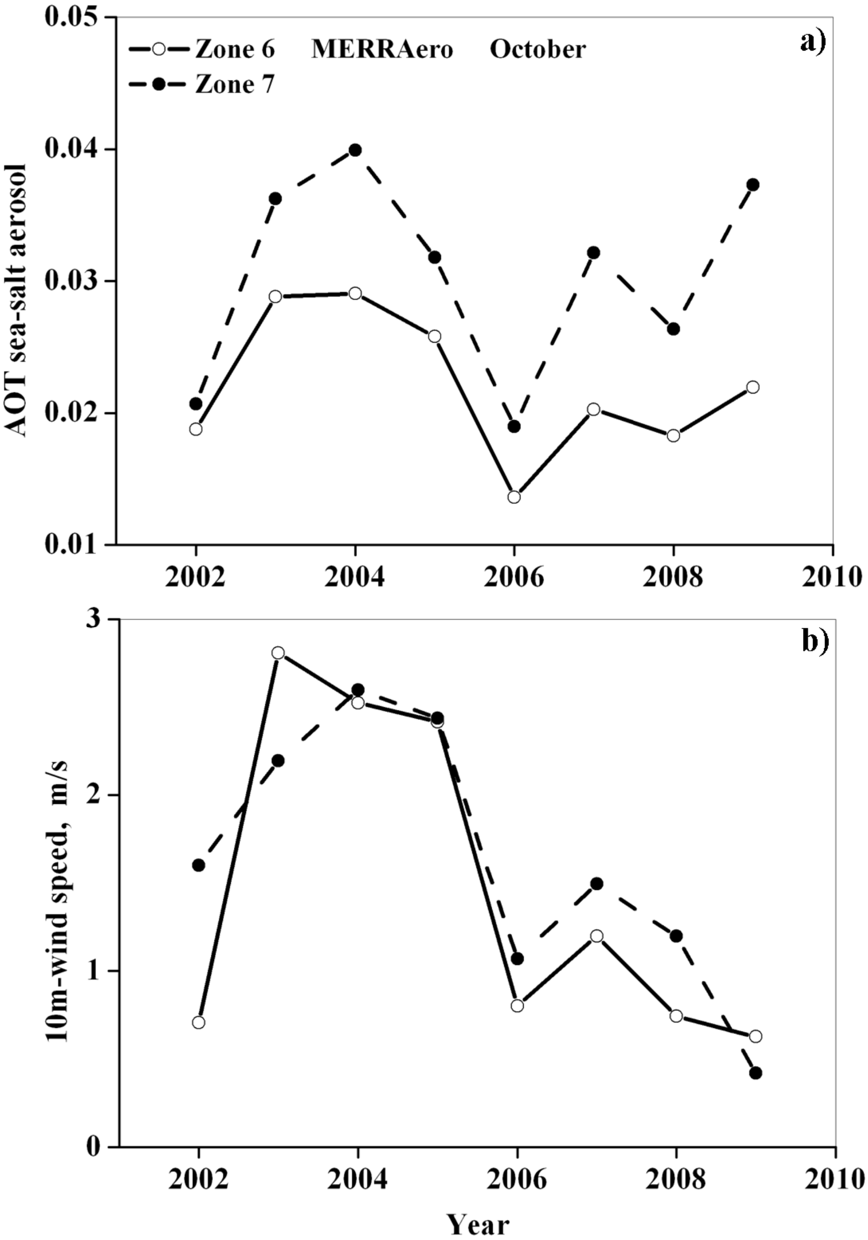

Figure 7. Year-to-year variations of (a) MERRAero AOT of sea-salt aerosols and (b) MERRA surface wind over north-west BoB (zones 6 and 7) in October.

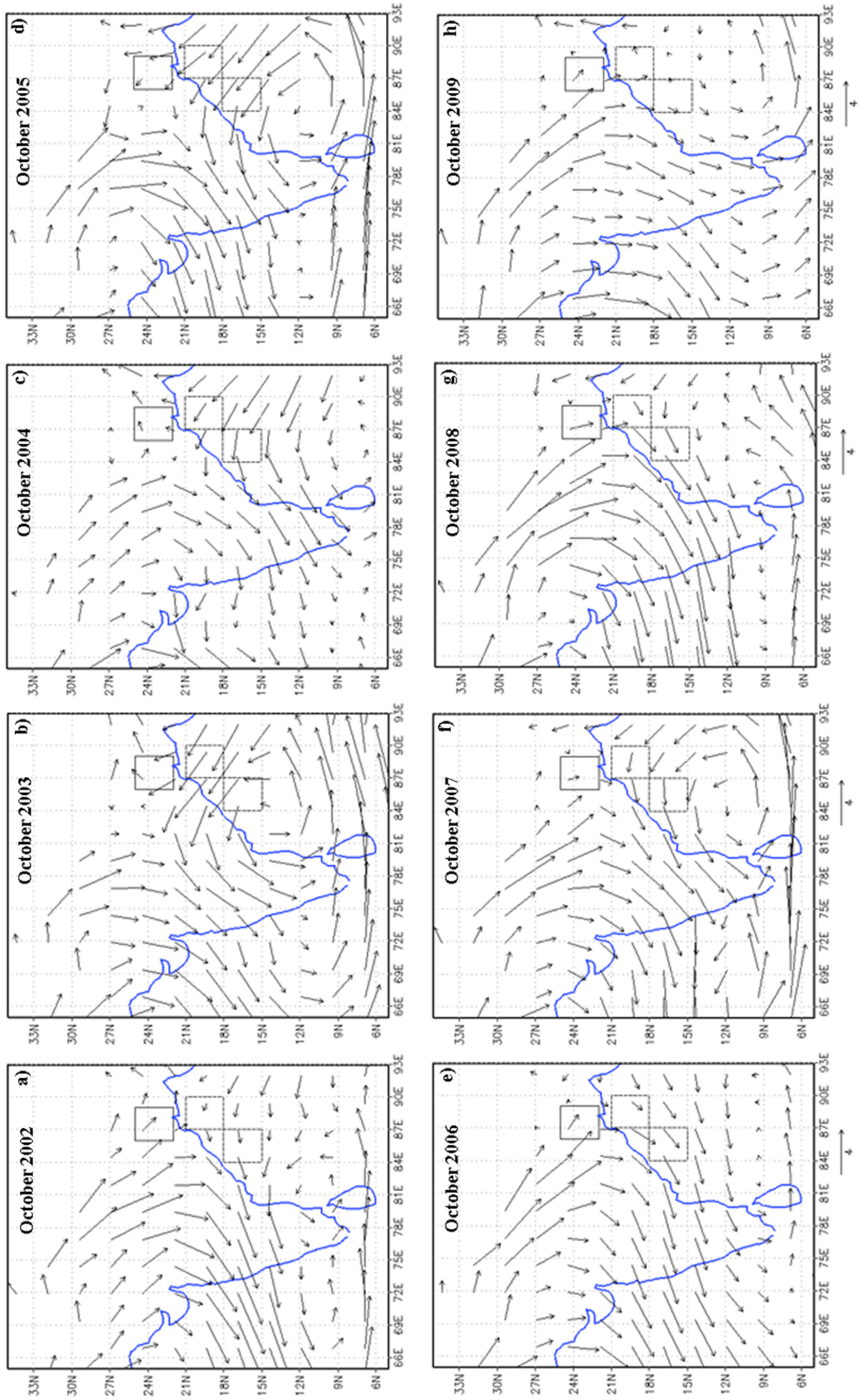

Figure 8. Spatial distributions of mean MERRA wind vectors of the 700-850 hPa layer in each October during the study period.

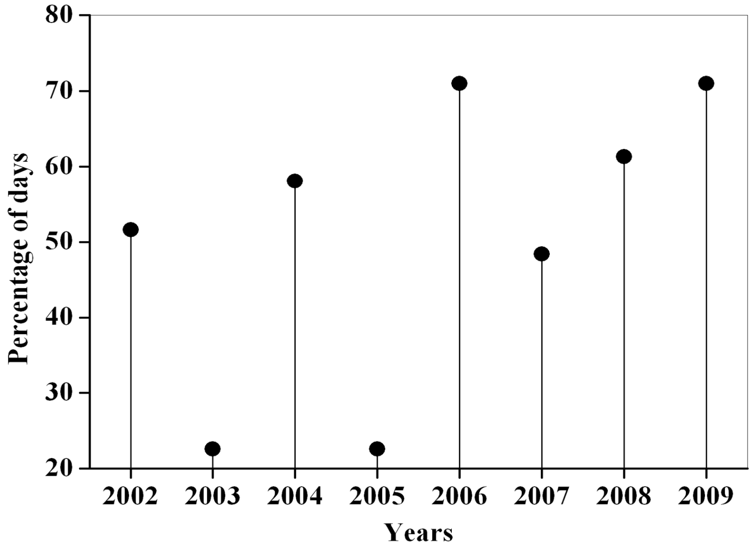

Figure 9. Numbers of days (in percentage form) in each October during the study period when prevailing wind (transporting air pollution) blew from the east of the Ganges basin (zone 5) to north-west BoB (zone 6).

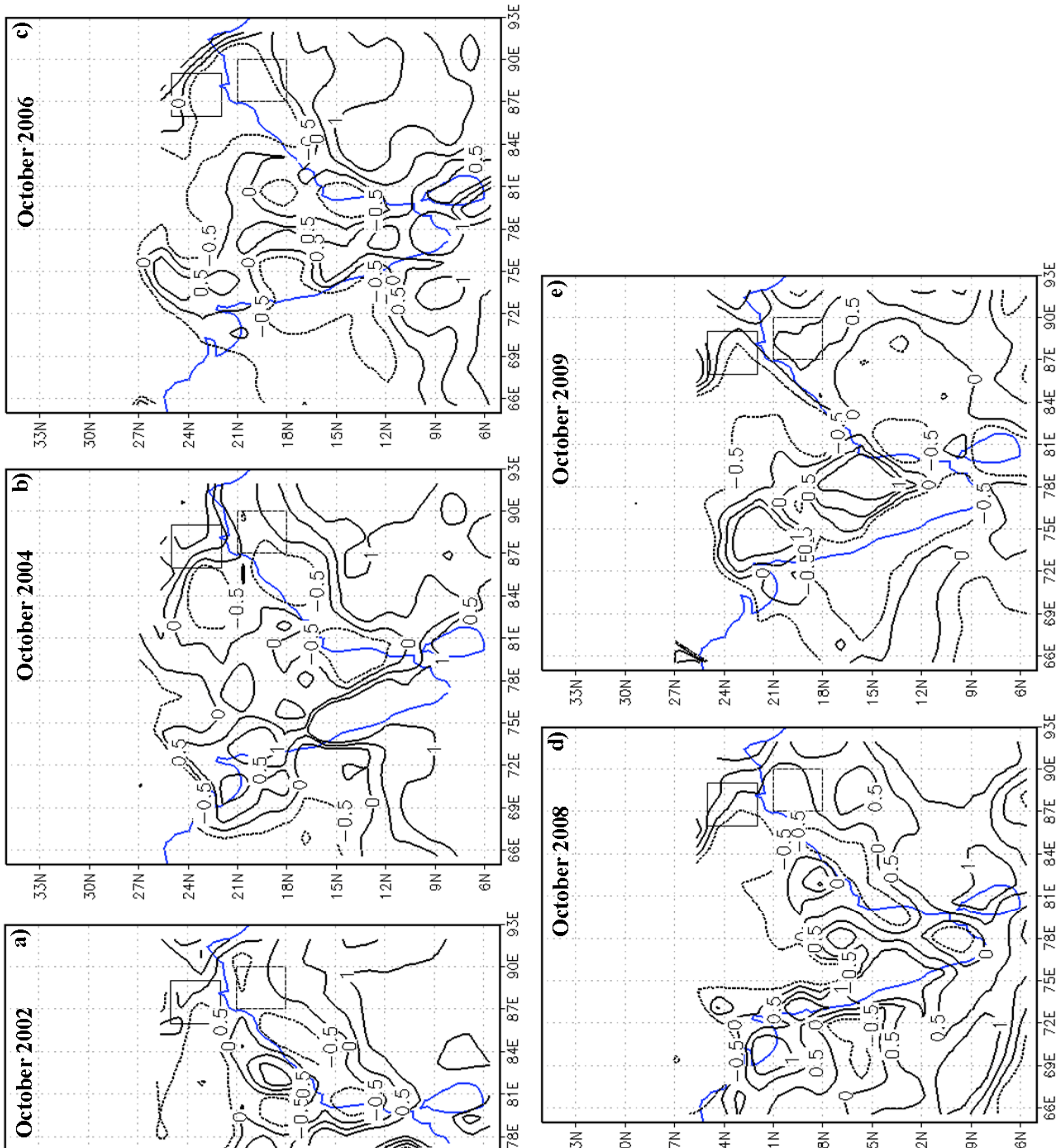

Figure 10. Spatial distributions of mean wind convergence (10^{-6} s^{-1}) of the 700-850 hPa layer for each October, when the number of days with prevailing winds, blowing from the east of the Ganges basin (zone 5) to north-west BoB (zone 6), exceeded 50%. MERRA wind reanalysis data were used.

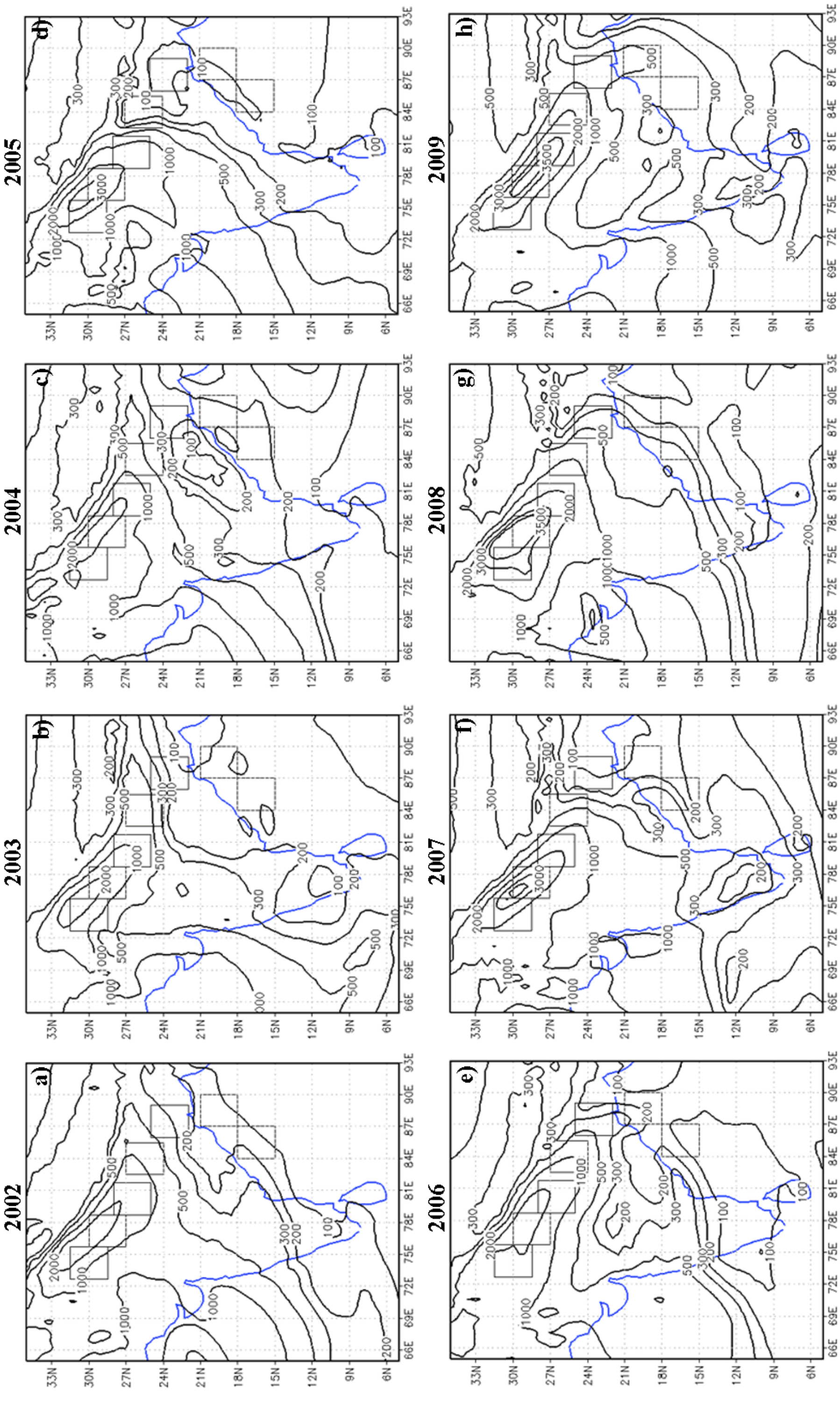

Figure 11. Spatial distributions of the absolute value of the magnitude of monthly integrated mass flux (kg m^{-1} $month^{-1}$) of aerosols (including sulfates, carbonates, and desert dust) in each October during the study period. The absolute value of the flux magnitude was obtained by the following expression: $((Fu)^2 + (Fv)^2)^{1/2}$, where Fu is the vertically integrated zonal mass flux and Fv is the vertically integrated meridional mass flux.

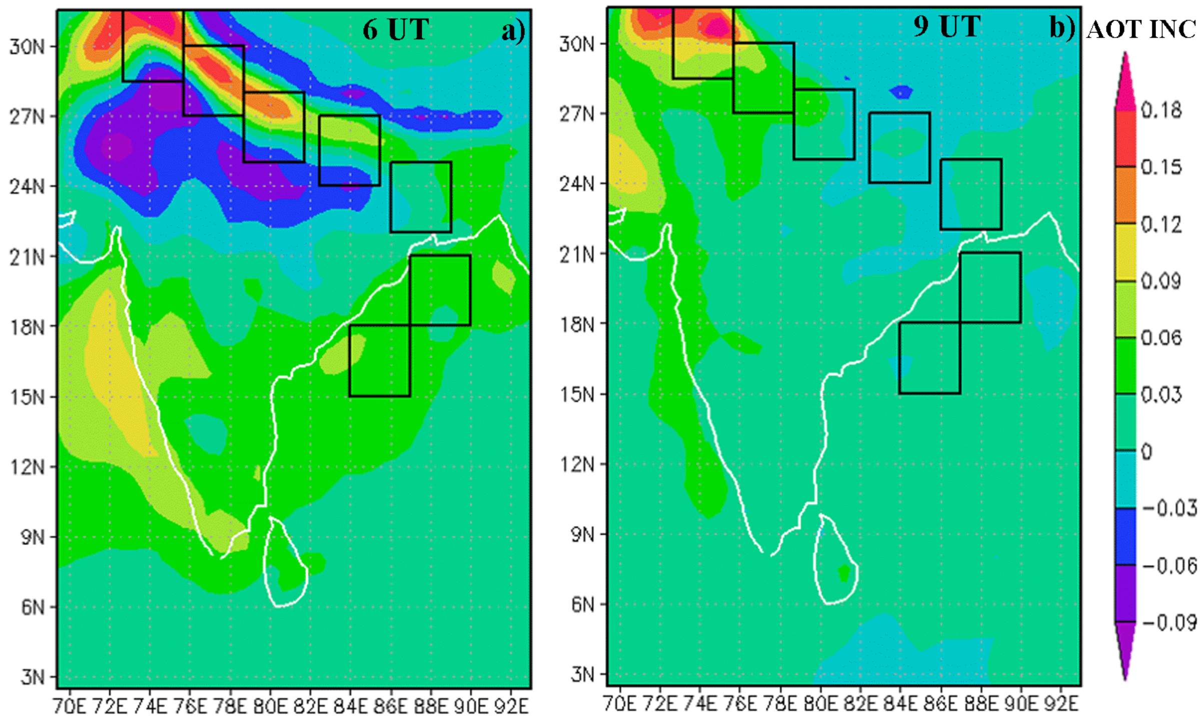

Figure 12. Spatial distributions of the eight year (2002 – 2009) mean AOT increments in October at (a) 6 UT and (b) 9 UT.

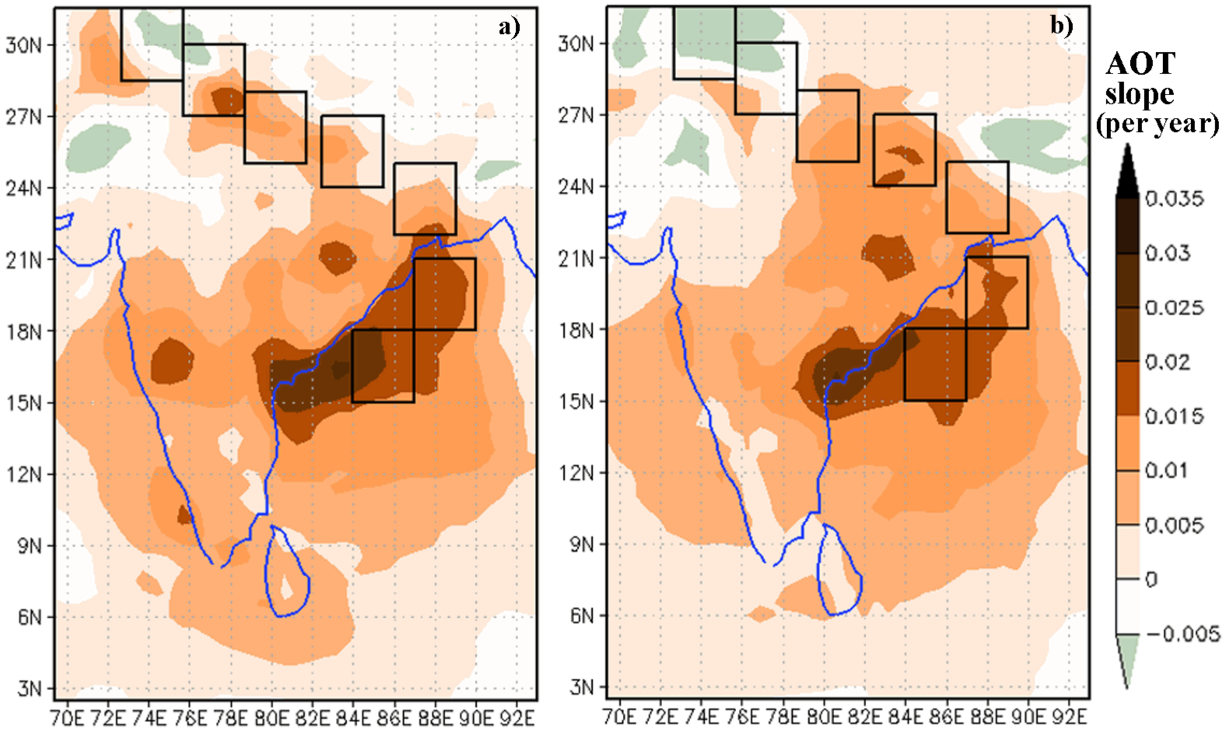

Figure 13. Spatial distributions of the eight year (2002 – 2009) MERRAero AOT trends (characterized by AOT slopes) in October at 6 UT: (a) with MODIS AOT assimilation and (b) without MODIS AOT assimilation.